JLAB E94010
Technical note
February 21, 2003

# Modifications to the QFS and RADCOR codes.

**v. 1.0**

K. Slifer
*Temple University,*
*Philadelphia, PA 19122, USA*
*E-mail: kslifer@temple.edu*

The **Q**uasi **F**ree **S**cattering fortran code of Lightbody and O'Connell is widely used to estimate counting rates in electron scattering. The unfolding code RADCOR is also widely used for radiative corrections to inelastic electron scattering data. We evaluate the reliability of the codes in the kinematic region of JLAB experiment E94010 and consider several modifications to the codes that were necessary. This document, as well as the fortran source codes are available at http://www.jlab.org/~slifer/codes.html

## Contents

## 1 Introduction

The QFS[1] model of J.W. Lightbody and J.S. O'Connell parametrizes electron scattering using five reaction channels in the impulse approximation:

1. Quasielastic scattering.
2. Two nucleon emission in the dip region.
3. $\Delta$ resonance electroproduction.
4. W = 1500 MeV resonance electroproduction.
5. W = 1700 MeV resonanace electroproduction.
6. Deep Inelastic Scattering.

There are three free parameters that the user may adjust:

1. $P_f$ : the Fermi momentum of the target nucleus.
2. Eps : the nucleon separation energy.
3. Epsd : the delta separation energy.

It has been used widely to estimate counting rates for inclusive electron scattering experiments such as those performed in JLAB Hall A.

## 2 Comparison to Data

To gauge the accuracy of the QFS model, we have made a comparison of the model prediction with available carbon cross section data from Saclay[3] and Slac[4] in the quasielastic and delta regions. For this study, the free parameters were set to:

- $P_f$ = 220 MeV
- EPS = 10 MeV
- EPSD = –10 MeV

The separation energy parameters were chosen solely to give good agreement with the data, while the Fermi momentum was chosen to be a reasonable value for carbon.

It was found that there is a strong $Q^2$ dependence that makes the calculation unreliable at low $Q^2$ (See Fig. 1). The new code includes an option to make a correction for this effect.

The limited available data in the $\Delta$ region was generally in good agreement (10%) with the model and as such no correction is attempted (See Fig. 2).

No comparison of higher resonances was performed due to the lack of available data.

## 3 Radiative Corrections

The original code allows for computation of both the $1^{st}$ order Born cross section and the radiated experimental cross section, although only internal radiative effects are taken into account. To extend the code to include external effects, we rewrote the subroutines that perform the radiation using the peaking approximation formalism of S. Stein [2] *et al.*

$$\begin{aligned}\left(\frac{d^2\sigma}{d\Omega dE_p}\right)_{exp} &= \left(\frac{R\Delta}{E_s}\right)^{bt'_b}\left(\frac{\Delta}{E_p}\right)^{bt'_a}\left[1-\frac{\xi/\Delta}{1-b(t'_b+t'_a)}\right]\tilde{\sigma}(E_s,E_p)\\ &+\int_{E_{Smin}}^{E_S-R\Delta}\tilde{\sigma}(E'_s,E_p)\left(\frac{E_s-E'_s}{E_pR}\right)^{bt'_a}\left(\frac{E_s-E'_s}{E_s}\right)^{bt'_b}\\ &\times\left[\frac{bt'_b}{E_s-E'_s}\phi\left(\frac{E_s-E'_s}{E_s}\right)+\frac{\xi}{2(E_s-E'_s)^2}\right]dE'_s\\ &+\int_{E_P+\Delta}^{E_{Pmax}}\tilde{\sigma}(E_s,E'_p)\left(\frac{E'_p-E'_p}{E'_p}\right)^{bt'_a}\left(\frac{(E'_p-E_p)R}{E_s}\right)^{bt'_b}\\ &\times\left[\frac{bt'_a}{E'_p-E_p}\phi\left(\frac{E'_p-E_p}{E'_p}\right)+\frac{\xi}{2(E'_p-E_p)^2}\right]dE'_p \qquad (1)\end{aligned}$$

where:

$$R=\frac{M_T+2E_s\sin^2(\theta/2)}{M_T-2E_p\sin^2(\theta/2)} \qquad (2)$$

$$\Delta = 10MeV \qquad (3)$$

$$\phi(v)=1-v+\frac{3}{4}v^2 \qquad (4)$$

$$b\simeq\frac{4}{3} \qquad (5)$$

$$t_r=\frac{1}{b}\frac{\alpha}{\pi}\left[\ln\frac{-q^2}{m^2}-1\right] \qquad (6)$$

$$T=t_b+t_a \qquad (7)$$

$$t'_b=t_b+t_r \qquad (8)$$

$$t'_a=t_a+t_r \qquad (9)$$

$$\eta = \ln(1440Z^{-2/3})/\ln(183Z^{-1/3}) \tag{10}$$

$$\xi = \frac{\pi m}{2\alpha}\frac{t_b + t_a}{(Z+\eta)\ln(183/Z^{1/3})} \tag{11}$$

$$\Phi(x) = \int_0^x \frac{-\ln|1-y|}{y}dy \tag{12}$$

$$E_{Pmax} = \frac{E_s}{1+\frac{E_s}{M}(1-\cos\theta)} \tag{13}$$

$$E_{Smin} = \frac{E_p}{1-\frac{E_p}{M}(1-\cos\theta)} \tag{14}$$

$$\tilde{\sigma}(E_s, E_p) = \tilde{F}(q^2)\sigma(E_s, E_p) \tag{15}$$

$$\tilde{F}(q^2) = 1 + 0.5772 \times bT + \frac{2\alpha}{\pi}\left[\frac{-14}{9} + \frac{13}{12}\ln\frac{-q^2}{m^2}\right] \tag{16}$$

$$-\frac{\alpha}{2\pi}\ln^2\left(\frac{E_s}{E_p}\right) + \frac{\alpha}{\pi}\left[\frac{1}{6}\pi^2 - \Phi(\cos^2\frac{\theta}{2})\right] \tag{17}$$

and $E_s$ ($E_p$) is the incident (scattered) electron energy.

Regarding the validity of the peaking approximation, we quote Tsai [8]:

> "...the tail from the elastic peak is large and long and its effect is felt all the way to the end of the spectrum, but the tails from the inelastic events are small and short and its effect is felt only by their neighbors. From the numerical examples given in MT [7] all versions of the peaking approximations give excellent results when the energy loss due to radiation is smaller than 10% of the electron energy. Hence the peaking approximation can be safely used when calculating the tail from the inelastic events."

In principle, the new code should reproduce the original qfs.f code radiated result if the target thicknesses before and after scattering ($t_b$ and $t_a$) are set to zero so that only internal radiative corrections are performed. To test this, we generated six spectra for $^3$He using the original and new code with T=0. Results are shown if Fig. 3. The incident energies and scattering angle (15.5°) correspond to the kinematics of experiment E94010 . The two codes agree exactly in the resonances and diverge slightly at large energy loss with the new code predicting a larger rate than the original.

To estimate the accuracy of the new code, we have radiated several QFS generated spectra for $^3$He at incident energies from 0.9 GeV to 5.1 GeV and at a scattering angle of 15.5 °. Typical radiation lengths of target material before and after scattering were $t_b = 0.007$ and $t_a = 0.04$ respectively. These

"experimental" cross sections are then unfolded using two available peaking approximation codes. ( See Figs. 4 to 9.) The first unfolding code **radcor.f**[5] is based on the formalism described in Guthrie Miller's thesis[6] and has been used extensively for past SACLAY and JLAB experiments. The code however makes several approximations based on the assumption that the thickness before and after scattering are equal. This is not a valid assumption when we consider the typical E94010 thicknesses mentioned above. The second code is a modification of the first code using the treatment prescribed by Stein[2] *et al.* It makes no assumptions regarding target thickness.

The output of both unfolding codes agree very well with the original model generated Born cross section in the resonance region. This gives us confidence in both the radiating code (nqfs.f) and the unfolding codes. The original radcor.f code however begins to diverge from the expected result in the large energy loss region($\nu \geq E_s/3$) as the incident energy increases. The modified code using the Stein formalism gives excellent results at all $\nu$ within a few percent.

Since the original model is folded using the Stein formalism, what we see here is the difference of the Miller and Stein approach in the unfolding peaking approximation combined with the effect of properly treating target thicknesses. It is reassuring to find that both approaches give the same result in the resonance region. The question of which peaking approximation is more accurate at large $\nu$ can only be answered by a comparison with the exact unfolding procedure. In the absence of such a study, we note that the Stein paper was written several years after the Miller thesis and includes several terms that are neglected in the Miller treatment.

## 4 References


1. J.W. Lightbody Jr, J.S. O'Connell, *Computers in Physics.* **2**, 57 (1988).
2. S. Stein *et al. Phys. Rev. D* . **12** 1884 (1975).
3. P. Barreau *et al.* Deep Inelastic Electron Scattering from Carbon. *Nucl. Phys. A* **402**, 515 (1983). and KEK preprint 198212108.
4. D. B. Day *et al. Phys. Rev. C* . **48** 1849 (1975) and D. B. Day private communication.
5. Fortran code **radcor.f**. Roy Whitney.
6. Guthrie Miller. "Inelastic Electron Scattering at Large Angles." SLAC Report 129(1971)
7. L.W. Mo and Y.S. Tsai. Rev. Mod. Phys. **41** 205 (1969).
8. Y. S. Tsai. "Radiative Corrections to Electron Scatterings." SLAC-PUB-848 (1971)

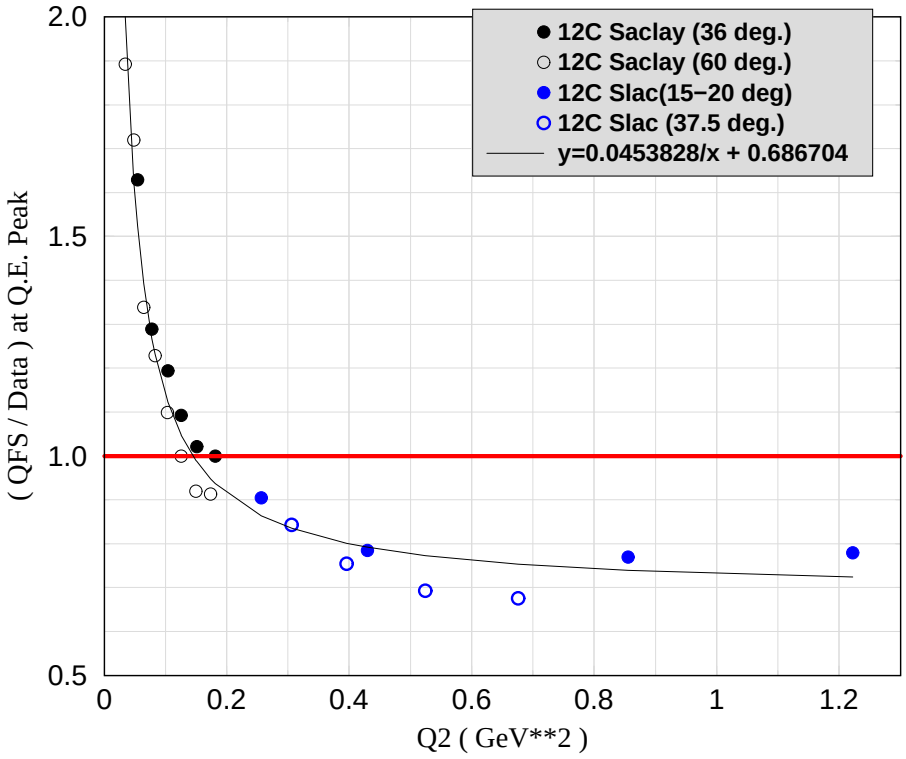


Figure 1: $Q^2$ dependence of the QFS model at the quasielastic peak for A=12. The data are from references [3] and [4]

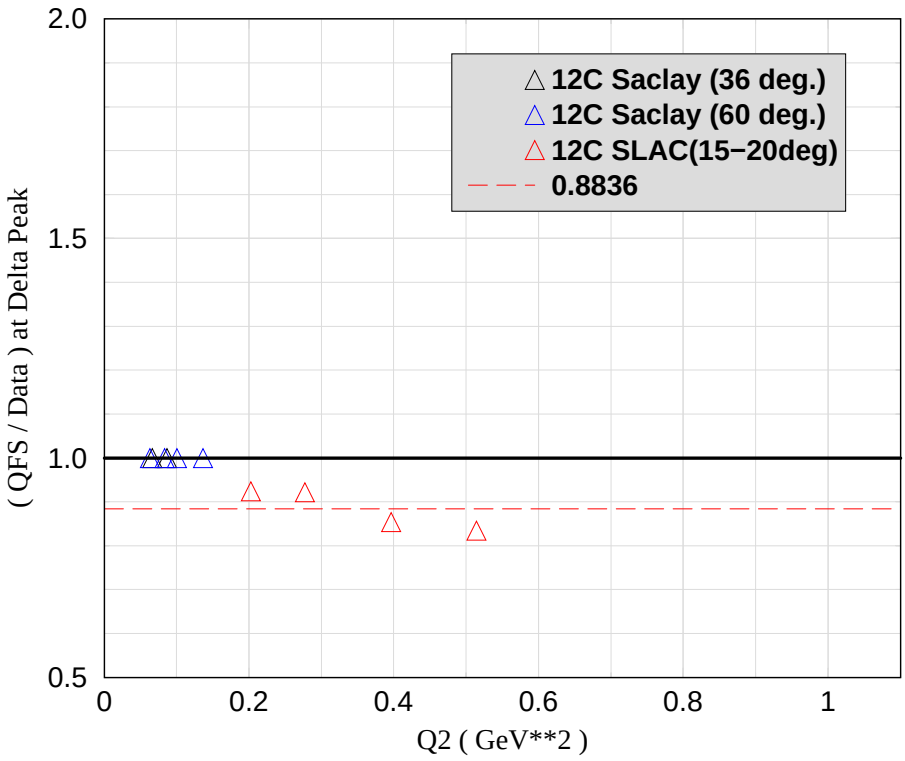


Figure 2: $Q^2$ dependence of the QFS model at the $\Delta$ peak for A=12. The data are from references [3] and [4]

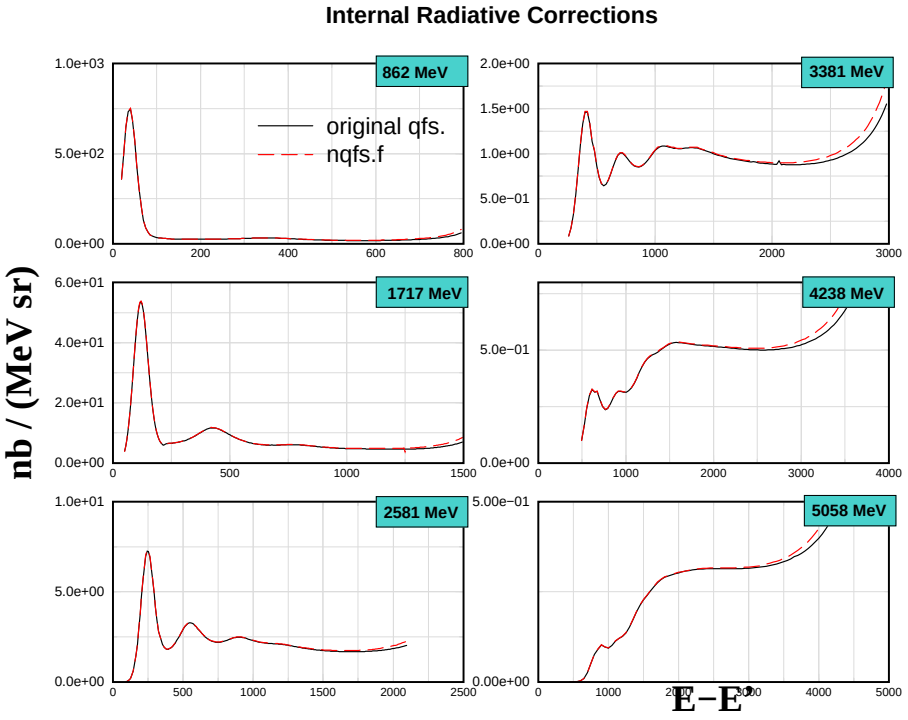


Figure 3: Comparison of internally radiative corrected cross section for original code and new code.

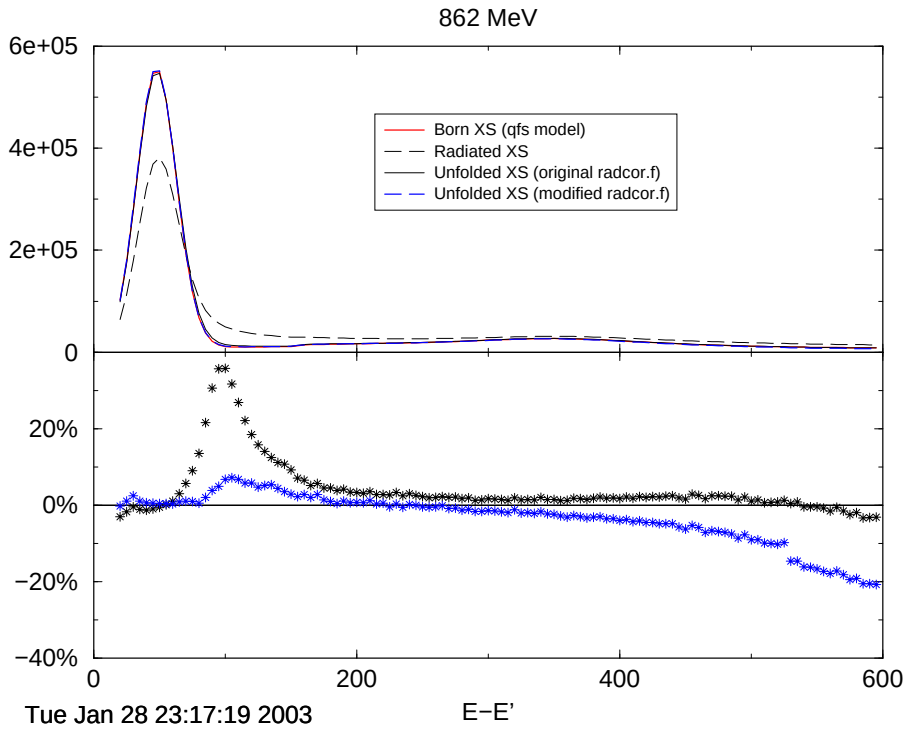


Figure 4: Top Panel: Cross sections. Bottom Panel: Percent difference of unfolded cross section from original model Born cross section. Black Star is original radcor.f code. Blue Star is modified radcor.f result.

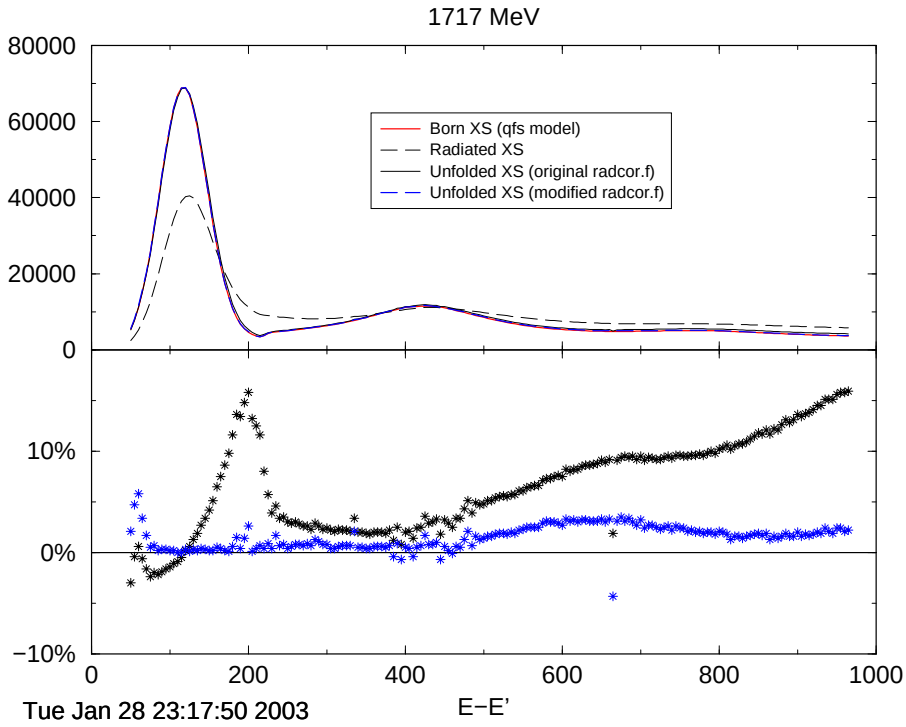


Figure 5: Top Panel: Cross sections. Bottom Panel: Percent difference of unfolded cross section from original model Born cross section. Black Star is original radcor.f code. Blue Star is modified radcor.f result.

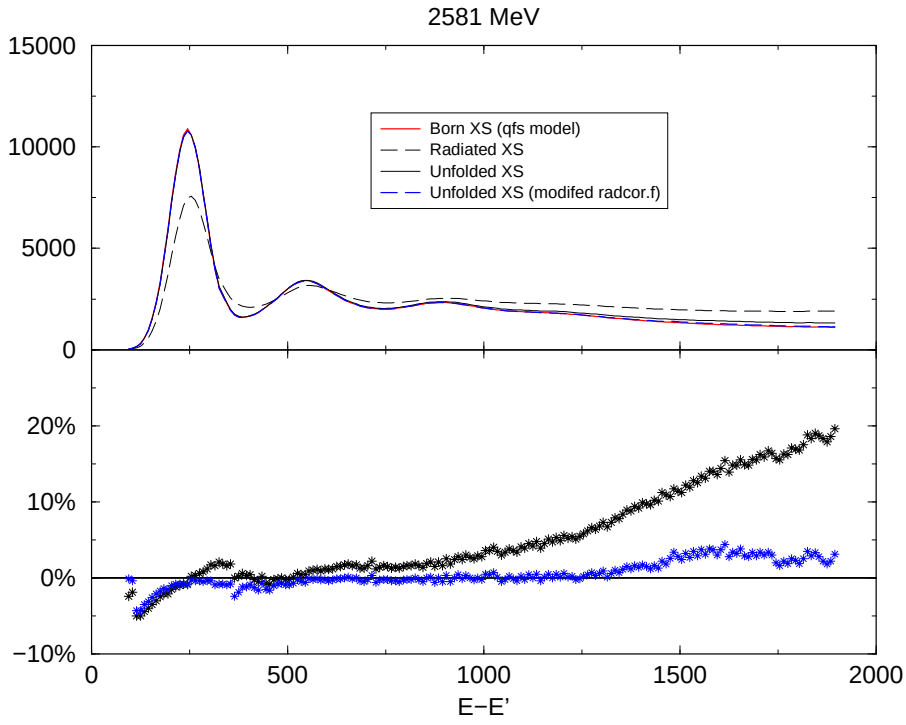


Figure 6: Top Panel: Cross sections. Bottom Panel: Percent difference of unfolded cross section from original model Born cross section. Black Star is original radcor.f code. Blue Star is modified radcor.f result.

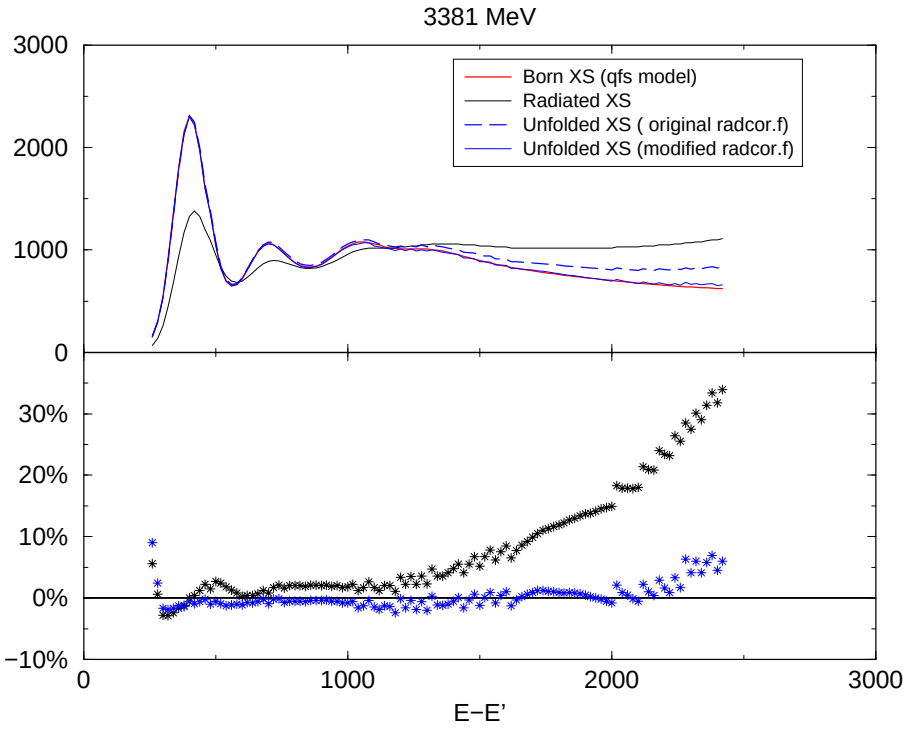


Figure 7: Top Panel: Cross sections. Bottom Panel: Percent difference of unfolded cross section from original model Born cross section. Black Star is original radcor.f code. Blue Star is modified radcor.f result.

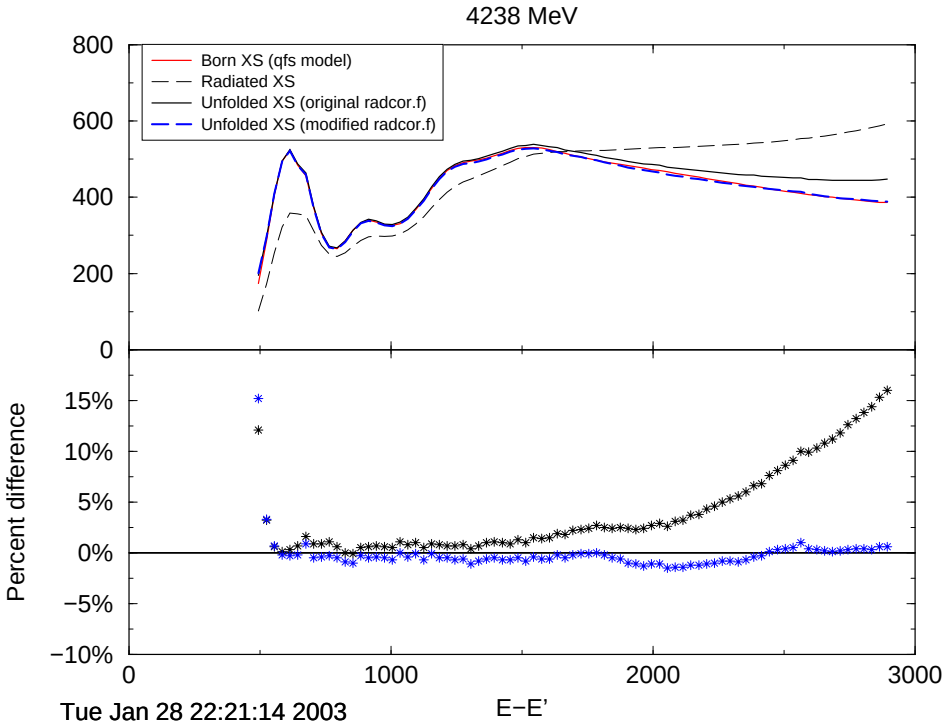


Figure 8: Top Panel: Cross sections. Bottom Panel: Percent difference of unfolded cross section from original model Born cross section. Black Star is original radcor.f code. Blue Star is modified radcor.f result.

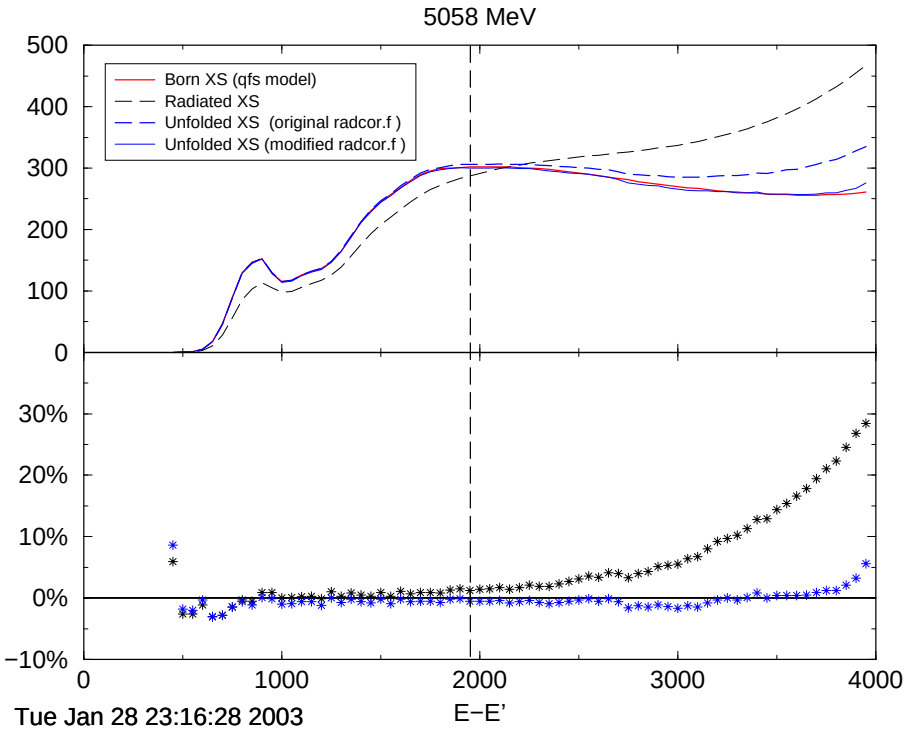


Figure 9: Top Panel: Cross sections. Bottom Panel: Percent difference of unfolded cross section from original model Born cross section. Black Star is original radcor.f code. Blue Star is modified radcor.f result.